Phytopathology Research

RESEARCH

Open Access

Detection and characterization of rice orange leaf phytoplasma infection in rice and *Recilia dorsalis*

Xiaofeng Zhang[1†], Zhenxi Ji[1†], Zhejun Huang[1†], Yibing Zhao[1], Huanqin Wang[1], Zhoumian Jiang[1], Zhanpeng Li[1], Hongyan Chen[1], Wenle Chen[2] and Taiyun Wei[1*]

Abstract

Phytoplasmas are small bacterial parasites that lack cell walls and are transmitted in a persistent-propagative manner by insect vectors. However, detailed multiplication patterns and movements of phytoplasmas within host plant and insect vector remain elusive. In this study, a specific antibody against the immunodominant membrane protein (Imp) of rice orange leaf phytoplasma (ROLP) was generated and subjected to the frozen section immune gold labeling assay, immune gold labeling microscopy, and immune fluorescence labeling assay to investigate how ROLP enters, propagates, and spreads in rice and its leafhopper vector *Recilia dorsalis* at the ultrastructural level. During acquisition and transmission by insect vectors, ROLPs could squeeze and penetrate the multiple membrane/tissue barriers such as microvilli, apical plasmalemma, and basal lamina in the intestines or salivary glands by endocytosis- and exocytosis-like mechanism. Furthermore, ROLP infection is restricted to the type IV and V cells of salivary glands. In contrast to the classical binary fission used by most bacteria, electron microscopy reveals that ROLP exploits an asymmetrical budding strategy to replicate in plant hosts and insect vectors. In this process, a cellular protrusion of ROLP forms a bud to reproduce the offspring by fission at the junction between the bud and the ROLP main body. These results clarify the infection characteristics of ROLP in rice and *R. dorsalis*, which will help guide the formulation of ROLP prevention and control strategies.

Keywords: Rice orange leaf phytoplasma, Transmission, Propagation, Rice, Insect vector

Background

The genus '*Candidatus* (*Ca.*) Phytoplasma' comprises a diverse group of bacteria that cause economically important insect-transmitted diseases around the world (Hogenhout et al. 2008b; Kumari et al. 2019; Namba 2019). Phytoplasmas are obligate parasites with a dual-host life cycle that alternates between plants and insects. In plants, phytoplasmas colonize the cytoplasm of vascular phloem cells that transport nutrients to growing plant tissues (Pagliari et al. 2016; Pagliari and Musetti 2019van Bel 2019). Sap-feeding insects that feed from the phloem, predominantly leafhoppers, planthoppers, and psyllids of the order *Hemiptera*, are often efficient phytoplasma vectors (Weintraub and Beanland 2006). Phytoplasmas are transmitted in a persistent manner and undergo a propagative and multiplicative cycle in their insect vectors, where they colonize the midgut and salivary glands (Weintraub and Beanland 2006; Hogenhout et al. 2008a). Koinuma et al. (2020) previously investigated the spatiotemporal dynamics of onion yellows

†Xiaofeng Zhang, Zhenxi Ji, and Zhejun Huang contributed equally to this work.

*Correspondence: weitaiyun@fafu.edu.cn

[1] State Key Laboratory of Ecological Pest Control for Fujian and Taiwan Crops, Institute of Plant Virology, Fujian Agriculture and Forestry University, Fuzhou 350002, Fujian, China
Full list of author information is available at the end of the article

phytoplasma in the leafhopper vector *Macrosteles striifrons* using immunofluorescence microscopy. Many studies have described the interactions of phytoplasma extracellular membrane proteins, such as antigenic membrane protein (Amp), immunodominant membrane protein (Imp), and variable membrane protein A (VmpA), with insect proteins such as actin microfilaments, ATP synthase, and surface glycoprotein (Galetto et al. 2011; Rashidi et al. 2015; Konnerth et al. 2016; Arricau-Bouvery et al. 2018; Abbà et al. 2019; Rossi et al. 2019). These interactions may enable the adhesion, entry, or movement of phytoplasmas in insect vectors. However, at the ultrastructural level, how phytoplasmas overcome membrane and tissue barriers of midgut and salivary glands during their acquisition and transmission by insect vectors remains unknown.

A more general unanswered question is how phytoplasmas propagate in plant hosts and insect vectors. Most bacteria rely on binary fission for propagation, but some species use other mechanisms, including formation of multiple intracellular offspring and stalked budding, to reproduce (Angert 2005; Eswara and Ramamurthi 2017). Phytoplasmas are small bacteria that lack cell walls and have been classified into 44 '*Ca.* Phytoplasma' species to date (Firrao et al. 2004; Lee 2004). The inability to culture phloem-inhabiting phytoplasmas is likely attributed to their reduced genomes, making them rely on host phloem or insect vector for survival and multiplication (Firrao et al. 2007; Sugio and Hogenhout 2012). The lack of cell wall and inability to culture in vitro contribute to the difficulty in understanding the propagation modes of phytoplasmas in host plants and insect vectors.

In this study, we used rice orange leaf phytoplasma (ROLP) and its leafhopper vector *Recilia dorsalis* to determine how phytoplasmas enter, propagate, and spread in insect vectors at the ultrastructural level. ROLP causes rice orange leaf disease (ROLD) and belongs to '*Ca.* Phytoplasma asteris', whose members are also the casual agents of some important diseases such as aster yellows, onion yellows, rhus yellows, mulberry dwarf, and paulownia witches' broom (Lee et al. 2000). ROLP was first identified in 1960 in Thailand; however, in the past decade, the disease caused by ROLP has become a threat to rice production, particularly in South China, India, Vietnam, Thailand, and the Philippines (Valarmathi et al. 2013; Li et al. 2015; Jonson et al. 2020; Ong et al. 2021). ROLP is mainly transmitted in a persistent-propagative manner by *R. dorsalis* with high efficiency and has evolved to adapt to the new vectors *Nephotettix cincticeps* and *Nephotettix virescens* (Li et al. 2015; Jonson et al. 2020). Here, we determined that ROLPs could penetrate membrane and tissue barriers in the intestines and salivary glands via endocytosis- and exocytosis-like mechanism. Our electron microscopy also revealed that ROLPs produce offspring by asymmetrical budding in plant hosts and insect vectors, which is potentially more suitable than other strategies for the wall-less ROLPs to produce abundant offspring.

Results

The specificity of antibodies against ROLP Imp

To investigate the infection process of ROLP in rice and *R. dorsalis*, the specific polyclonal antibodies against Imp were generated. A gene encoding Imp of ROLP was cloned and sequenced. The ROLP *Imp* gene has an open reading frame (ORF) of 456 nt and encodes a protein of 155 aa, sharing high identity (95.2%) with Imp proteins from several phytoplasmas including maize bushy stunt phytoplasma (WP_069028105.1), aster yellows phytoplasma (WP_130427454.1), rapeseed phyllody phytoplasma (QKX95641.1), chrysanthemum yellows phytoplasma (WP_034172217.1), '*Chrysanthemum coronarium*' phytoplasma (WP_011160959.1), '*Elaeagnus angustifolia*' witches' broom phytoplasma (MBT1576836.1), porcelain vine witches' broom phytoplasma (WP_219475381.1), mulberry dwarf phytoplasma (WP_227807050.1), and hydrangea phyllody phytoplasma (WP_212775527.1) (Additional file 1: Figure S1).

Combined with the analyses of hydrophilicity and antigenicity, five regions of Imp were chosen for peptide synthesis and subsequent generation of antibody (Fig. 1a). The specificity of polyclonal antibodies was tested via Western blotting assay. The *E. coli*-expressed Imp protein was purified and served as positive control. The results showed that the antibody against peptides at 56–69 aa named as Imp2 could specifically recognize Imp protein in samples of ROLP-infected rice and *R. dorsalis* (Fig. 1a). This indicates that antibody Imp2 can be applied to the detection of ROLP and other phytoplasmas.

The distribution of ROLPs with various morphologies in rice cells

To visualize the distribution of phytoplasmas in rice tissues, rice leaves with ROLD symptoms were sliced and embedded in freezing medium, serially sectioned, and immunohistochemically stained using Imp2 antibody conjugated with rhodamine. Under confocal microscope, the specific signals indicating the location of ROLP were either around the plasma membrane of sieve tube cells or filling the whole cells (Fig. 1b). To obtain the details of ROLP distribution in rice cells, the immunoelectron microscopic study with Imp2 antibody was performed. The results showed that plenty of thalli around with gold particles were found in sieve tube cells and companion cells, similar to phytoplasma previously reported

(Fig. 1c). No phytoplasmas were observed in asymptomatic controls.

Immunoelectron microscopy showed that a mass of ROLPs with varying shapes were observed in the sieve element of leaf samples (Fig. 1d I). ROLPs with sizes ranging from 50 to 1100 nm in diameter were bounded by a unit membrane containing large masses of filamentous flexuous threads and cytoplasmic cylindrical inclusions. Small electron dense spore-like virus particles with a diameter of 30–100 nm, also specifically labeled by golden particles, were found to attach to the membrane of ROLPs (Fig. 1d II–VII).

Infection route of ROLPs within the insect vector *R. dorsali*

Phytoplasmas acquired by insect vectors from diseased plants generally establish their initial infection in the insect intestine, and from there they are subsequently disseminated to the hemolymph, and finally establish in the salivary glands, where they are discharged with saliva (Weintraub and Beanland 2006; Hogenhout et al. 2008b).

To trace the infection route of ROLP in its vector, we investigated the distribution of ROLPs in *R. dorsali* at different days post-first access to diseased plants (padp) using immunofluorescence microscopy. No signal for the ROLP antigen was observed in the alimentary canal and salivary gland from the *R. dorsalis* fed on healthy rice (Fig. 2a, g). At 7 days padp, ROLP infection was first observed in a few epithelial cells of the filter chamber in about 23% of insects tested, suggesting that ROLPs ingested by *R. dorsalis* from diseased rice plants had crossed the microvilli into the intestinal epithelium (Fig. 2b, c and Table 1). At 14 days padp, ROLP infection had spread to the midgut epithelium in 50% of insects tested (Fig. 2d and Table 1). ROLP infection was first observed in the cytoplasm of type IV and V cells of salivary glands in about 6% insects tested, although ROLPs were also observed to attach to the cell surface of type IV and V salivary cells (Fig. 2h and Table 1). At this time, ROLP infection was also observed in the hemolymph of infected insects (Fig. 2l), suggesting that ROLP could efficiently spread from the alimentary system to salivary glands via the hemolymph. At 28 days padp, ROLPs could be extensively observed in the epithelium and visceral muscles throughout the alimentary system (Fig. 2e, f). At 21 and 28 days padp, ROLP infection had spread throughout type IV and V salivary cells, suggesting that ROLPs were specifically propagated in type IV and V salivary cells (Fig. 2i–k). Taken together, our results suggested that ROLP first infected epithelial cells of the filter chamber before proceeding to the whole alimentary system, and was then released into the hemocoel, from where ROLP finally spread into the salivary glands.

To confirm the results of immunofluorescence microscopy, we quantified the titers of ROLPs in the whole-body of *R. dorsalis* using quantitative PCR (qPCR) assay. At 7, 14, 21, and 28 days padp, total DNA from each ROLP-infected *R. dorsalis* was purified and subjected to qPCR test. Accumulation of ROLPs in *R. dorsalis* increased gradually from 7 to 28 days padp (Fig. 2m). ROLP titers remained low or undetectable at 7 days padp, and then multiplied in a fast rate between 7 and 21 days padp. Rates of replication then slowed again from 21 to 28 days padp (Fig. 2m). These results were consistent with the results of Western blotting assay with antibody against the ROLP membrane protein Imp (Fig. 2n). Thus, ROLP propagation showed an exponential phase of growth from 7 to 21 days padp and then entered the stationary growth phase.

Process for ROLPs to overcome transmission barriers in the insect vector *R. dorsalis*

During transmission, phytoplasmas must overcome multiple tissue and membrane barriers in insect bodies (Hogenhout et al. 2008b; Pagliari and Musetti 2019). We first observed how ROLP enters the intestinal epithelium from the lumen after acquisition from diseased rice plants. The alimentary canal of *R. dorsalis* is composed of a single layer of epithelial cells with microvilli on the lumen side, which are covered by a perimicrovillar membrane (Fig. 3a). At 7 days padp, electron microscopy

(See figure on next page.)

Fig. 1 The specificity of antibodies against Imp and detection of ROLP infection in rice tissues. **a** Schematic illustration of the peptide design of Imp (17 kDa). Western blotting analyses showing specificity of antibodies of Imp2, Imp4, and Imp5. Total proteins from *E. coli* strain expressing Imp, ROLP-infected or healthy leafhopper, or ROLP-infected or healthy rice were separated by SDS-PAGE. **b** Immunofluorescence micrographs showing the distribution of ROLPs in the phloem of rice leaves with typical ROLD symptoms. Frozen slices from healthy or ROLP-infected rice tissues were immunolabeled with Imp-specific antibody directly conjugated with rhodamine (Imp-rhodamine, red) and then examined by immunofluorescence microscopy. Ve, vessel; ST, sieve tube. Scale bars, 20 μm. **c** Electron micrographs showing the distribution of ROLPs in the vascular bundles of ROLP-infected rice leaves. Panel i, phloem cells of ROLP-infected rice leaves. Panel ii is the enlarged image of the boxed area in panel i, showing ROLP-infected companion cells. Scale bars, 10 μm (i) and 500 nm (ii) **d** Electron micrographs of ROLP-infected sieve tube cells of rice. Panels II–VII are the enlarged images of the ROLP-infected cells in panel I. Panels IV–VII, morphologically different small virus-like particles which were specifically labeled by gold particles. Mes, mesophyll; PP, phloem parenchyma; SE, sieve elements; ST, sieve tube; Ve, vessel. Scale bars, 500 nm (i) and 60 nm (ii–vii)

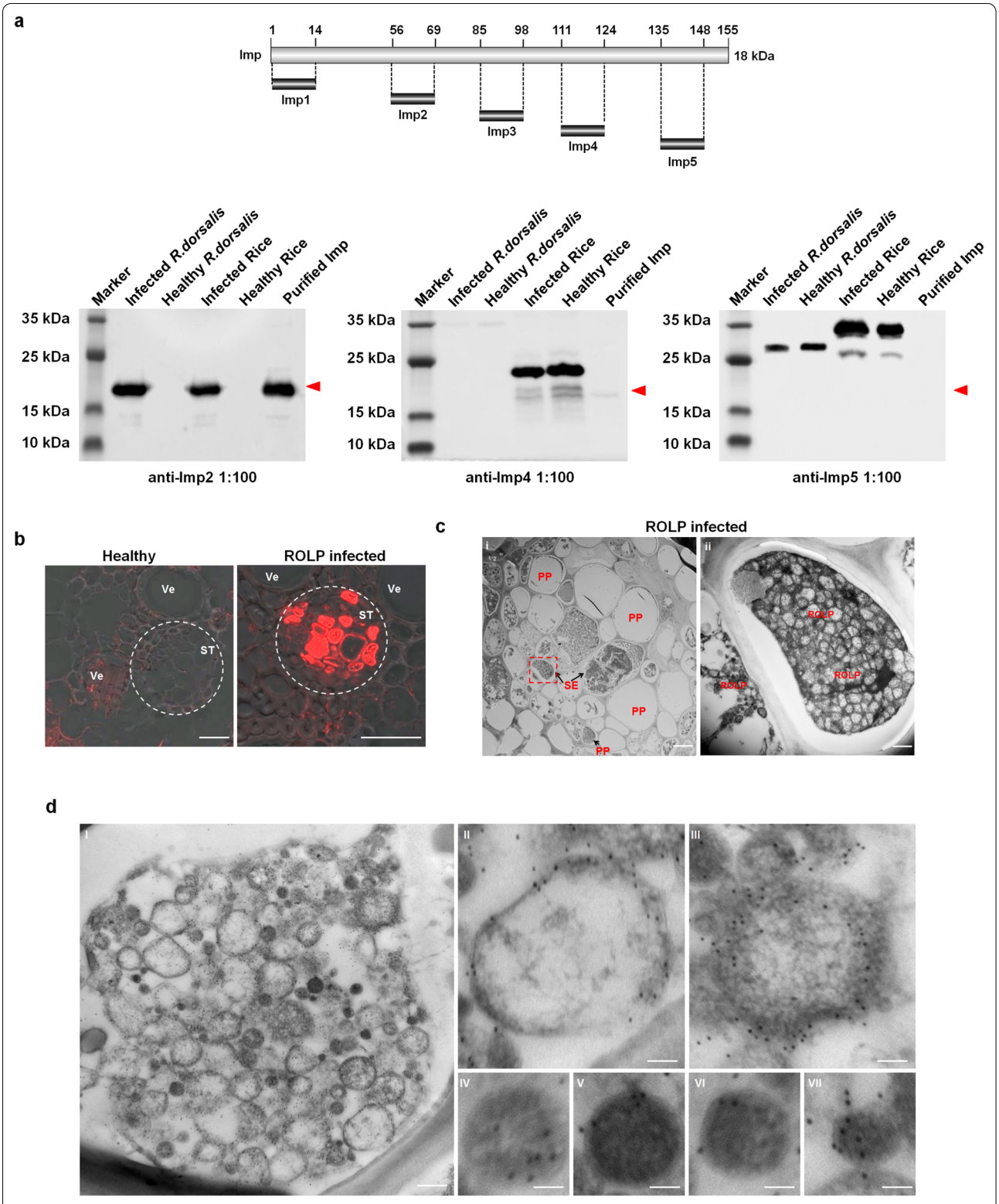

Fig. 1 (See legend on previous page.)

showed that ROLPs of various sizes acquired from diseased rice plants had accumulated abundantly in the intestinal lumen (Fig. 3b, c). These ROLPs initially attached to the perimicrovillar membrane and then passed through the brush border of microvilli by inducing its membrane curvature (Fig. 3d–g). After attachment to the apical plasmalemma of intestinal epithelial cells, ROLPs penetrated the membrane by an endocytosis-like mechanism (Fig. 3h–j).

The intestinal epithelial cells of *R. dorsalis* are lined with basal lamina and visceral muscles on the hemocoel side, which are covered with the serosal barrier (Fig. 3a). We next used electron microscopy to investigate how ROLPs overcome the intestinal release barrier to spread into the hemolymph. At 21 days padp, abundant ROLPs were distributed along the basal lamina or visceral muscles lining the midgut epithelium (Fig. 4a). Careful observations revealed that, after attachment to the basal lamina, ROLPs could propel the extension of the basal lamina (Fig. 4b). This process finally led to the passing of ROLPs through the basal lamina (Fig. 4c). Furthermore, ROLPs could align along the serosal barrier on the surface of visceral muscles (Fig. 4d). ROLPs squeezed and then penetrated the serosal barrier to release into the hemolymph by an exocytosis-like mechanism (Fig. 4e–h).

R. dorsalis salivary gland cells are surrounded by basal lamina on the hemolymph side and filled with abundant apical plasmalemma-lined cavities, where saliva is stored. We next investigated how ROLPs overcome the salivary gland barrier to enter into rice plants via electron microscopy at 14 and 28 days padp. At 14 days padp, ROLPs of various sizes in the hemolymph could attach to and then penetrate the basal lamina, finally moving into salivary cells (Fig. 4i, j). At 28 days padp, abundant ROLPs in the cytoplasm of secretory cells were observed to attach to and squeeze the apical plasmalemma towards the cavity, which was followed by the curvature of the apical plasmalemma (Fig. 4k–n). Finally, ROLPs were released into salivary cavities (Fig. 5). Taken together, these results revealed that ROLPs penetrate membrane and tissue barriers encountered in the intestines or salivary glands by endocytosis- and exocytosis-like mechanism, facilitating efficient phytoplasma transmission by insect vectors.

Reproduction of ROLPs in the insect vector *R. dorsalis*

We next investigated how ROLPs propagate during the exponential growth phase in midgut epithelial cells and salivary gland cells using electron microscopy. At 14 days padp, ROLPs initiated an active propagation process to produce offspring after their entry into midgut epithelial cells. Electron microscopy showed that one ROLP mother cell produced one daughter cell, which then produced more offspring, forming grapelike clusters (Fig. 6a–d). Eventually, ROLPs of various sizes were dispersed throughout the cells of the midgut or salivary gland (Fig. 6e–g).

We then observed how ROLPs produced offspring in the cells of the midgut or salivary gland using electron microscopy. ROLP cytoplasm was bounded by a standard gram-positive envelope consisting of an inner membrane and an outer membrane, with its center occupied by large masses of flexuous cytoplasmic chromosomal DNA. Electron microscopy showed that ROLPs generally exploited an asymmetrical budding strategy to produce offspring. This process began with the extension of the ROLP envelope at the cell pole, which then formed a protrusion from the cell surface (Fig. 6h). The protrusion envelope was consistently lined with ROLP membrane (Fig. 6i). Subsequently, the cellular protrusion became enlarged for the onset of bud formation (Fig. 6j–l). The bud finally separated from the mother cell by fission at the mother cell-bud junction (Fig. 6l). Thus, the bud formed by gradual expansion of ROLP membranes to produce a new

(See figure on next page.)

Fig. 2 Infection route of ROLPs in the internal organs or tissues of its leafhopper vector *R. dorsalis*. Second-instar *R. dorsalis* nymphs were fed on ROLP-infected rice leaves for 4 days and then transferred to healthy rice seedlings. At different days post-first access to diseased plants (padp), organs or tissues dissected from insects were immunolabeled with Imp-rhodamine (red) and actin dye phalloidin-Alexa Fluor 647 (blue), then examined using immunofluorescence microscopy. **a** Alimentary canal of *R. dorsalis*. **b** Initial infection by ROLPs in the filter chamber (arrow) as early as 7 days padp. Panel ii is the enlarged image of the boxed area in panel i. **c** Extensive ROLP infection in the filter chamber at 7 days padp. **d** Extensive ROLP infection in the midgut epithelial cells at 14 days padp. Panels ii and iii are the enlarged images of boxed areas in panel i and ii, respectively. **e**, **f** Extensive ROLP infection in midgut epithelial cells (**e**) and visceral muscles (**f**) at 28 days padp. Panel ii is the enlarged image of boxed area in panel i. **g** Salivary gland of *R. dorsalis*. **h** Initial infection of ROLPs in type IV and V salivary cells at 14 days padp. Panel ii is the enlarged image of boxed area in panel i. **i**–**k** Extensive ROLP infection in type IV and V salivary cells at 21 or 28 days padp. **l** The distribution of ROLPs in the hemolymph from healthy or ROLP-infected insects. **m** Time course analysis of ROLP accumulation in infected insects by qPCR assay. At 7, 14, 21, and 28 days padp, a group of 15 *R. dorsalis* individuals were collected. Each insect was ground individually for DNA purification. Only ROLP-positive samples were used to measure phytoplasma titer. *P* values were estimated using Tukey's honest significant difference (HSD) test. * $P < 0.05$, ** $P < 0.01$. **n** ROLP Imp protein accumulation in infected insects at different days padp, as detected by Western blotting assay with Imp-specific antibody (Imp2). Actin was used as a loading control. amg, anterior midgut; ec, epithelial cell; es, esophagus; fc, filter chamber; mmg, middle midgut; mt, malpighian tubule; pmg, posterior midgut; sg, salivary gland; vm, visceral muscle. Scale bars, 100 μm (**a**–**k**) and 5 μm (**l**)

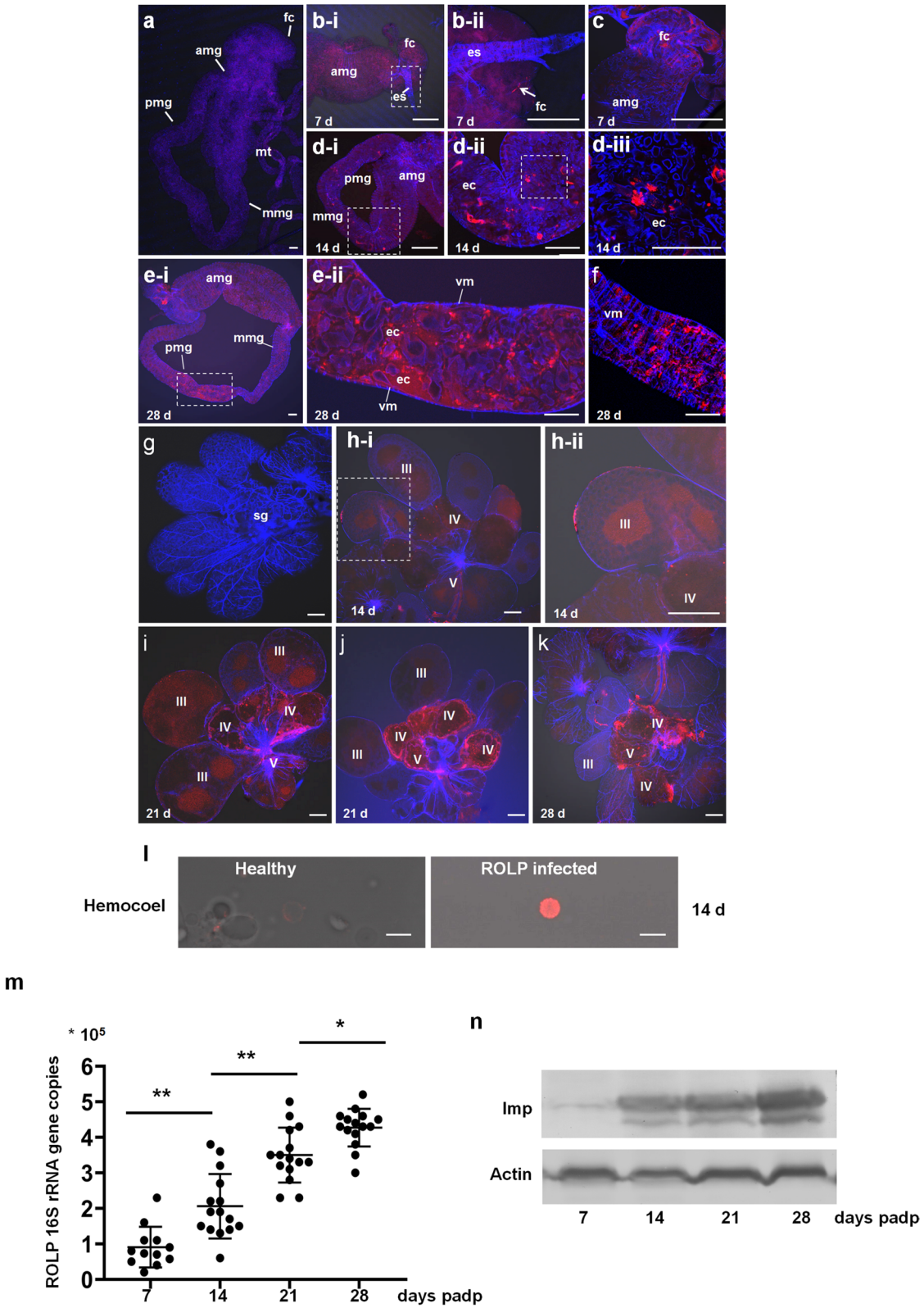

Fig. 2 (See legend on previous page.)

Table 1 Occurrence of ROLP Imp antigen in various tissues of *R. dorsalis* at different days post-first access to diseased plants (padp)

Days padp	No. of positive insects against ROLP antigen in specified tissues ($n = 30$/day)					
	Fc	Amg	Mmg	Pmg	He	Sg
7	7	5	0	0	0	0
14	15	12	7	5	6	2
21	19	18	17	15	16	14
28	24	24	24	23	24	20

Second-instar nymphs of *R. dorsalis* were fed on ROLP-infected rice plants for 4 days and then transferred to healthy rice seedlings. After different periods of time following their exposure to diseased plants, the internal organs of 30 individuals were immunolabeled with ROLP antigen and counted. Amg, anterior midgut; Fc, filter chamber; He, hemolymph; Mmg, mid-midgut; Pmg, posterior midgut; Sg, salivary gland

daughter cell (Fig. 6m). ROLPs also underwent a similar budding process to produce small daughter bacteria in the cytoplasm of vascular phloem sieve cells of ROLP-infected rice leaves (Additional file 1: Figure S2). Imp antibody could specifically label the membranes of buds and mother cells in ROLP-infected rice or leafhopper cells (Fig. 6h–m and Additional file 1: Figure S2). Thus, ROLP uses a conserved budding mechanism to reproduce in the plant host and insect vector (Fig. 6n).

Discussion

Phytoplasmas, which infect various plants including several economically important crops and vegetables, represent a severe threat to agriculture. They are transmitted by different leafhoppers, planthoppers, and psyllids in a persistent manner (Hogenhout et al. 2008b; Kumari et al. 2019; Namba 2019). Understanding their multiplication patterns and distributions in both plant and insect hosts will provide cues to develop novel control strategies. In the present study, using immunofluorescence and immunoelectron microscopy with an Imp-specific antibody, we provided the details of ROLP distribution in both rice and leafhopper and how ROLP overcomes diverse barriers in leafhopper.

Due to the extreme difficulty of culturing phytoplasmas in vitro and their obligate nature like wall-less and obligate phloem infection, the technologies suitable for investigations of phytoplasma morphology and distribution in host tissues, especially in plant tissues were limited (Galetto et al. 2011). In this study, a new immunofluorescence labeling assay based on the frozen rice tissue sections was developed to study the ROLP localization, which is less time-consuming and more convenient for sample preparation and observation compared with electron microscopy. What is more, with antibodies against different rice cell components, this method may open a way to study the subcellular localization of phytoplasma.

Electron microscopy has been frequently used to examine the temporal localization of phytoplasma with obvious limitations. For example, it cannot distinguish among different phytoplasmas, or different forms of phytoplasmas during proliferation. In our experiment, using a specific antibody against ROLP membrane protein Imp (Imp2), we observed the morphology of ROLPs in rice and leafhopper tissues at the ultrastructural level. Like other phytoplasmas, ROLPs varied in form, size, and degree of density of contents, spanning from small, dense virus-like particles (30–100 nm in diameter) to large, spherical of filamentous organisms (up to 1100 nm in diameter). One of the common forms has spherical electron lucent cytoplasmic region bound by a trilaminar unit membrane and occupied by fibrils resembling those of DNA. What is more important, we found some virus-like particles attached to the membrane of mature ROLPs were also specifically labeled by the gold particles, which represented an immature form of ROLP in the budding process of multiplication. These virus-like particles were also found in other phytoplasma-infected plant cells like aster yellows phytoplasma. However, the functions of these small particles involved in cell-to-cell movement and systemic movement of ROLP are worth further investigations.

(See figure on next page.)

Fig. 3 Electron micrographs showing the entry of ROLPs into the intestinal epithelium of *R. dorsalis*. **a** Intestinal epithelium, showing microvilli on the lumen side and basal lamina covered with muscle fibers and serosal barrier on the hemocoel side. **b** ROLP distribution in the gut lumen. ROLP-infected intestines were incubated with Imp-specific antibody and then with 15-nm gold particle-conjugated goat antibody against rabbit IgG as secondary antibody. **c**–**j** Process for entry of ROLPs from the gut lumen into epithelial cells by successively passing through the perimicrovillar membrane (**c**–**e**), microvilli (**f**, **g**), and apical plasmalemma (**h**–**j**). Arrows indicate ROLPs. AP, apical plasmalemma; EC, epithelial cell; GL, gut lumen; MV, microvilli; PM, perimicrovillar membrane; SB, serosal barrier. Black arrows indicate gold particles. Red arrows indicate ROLPs. Scale bars, 2 μm (**a**) and 200 nm (**b**–**j**)

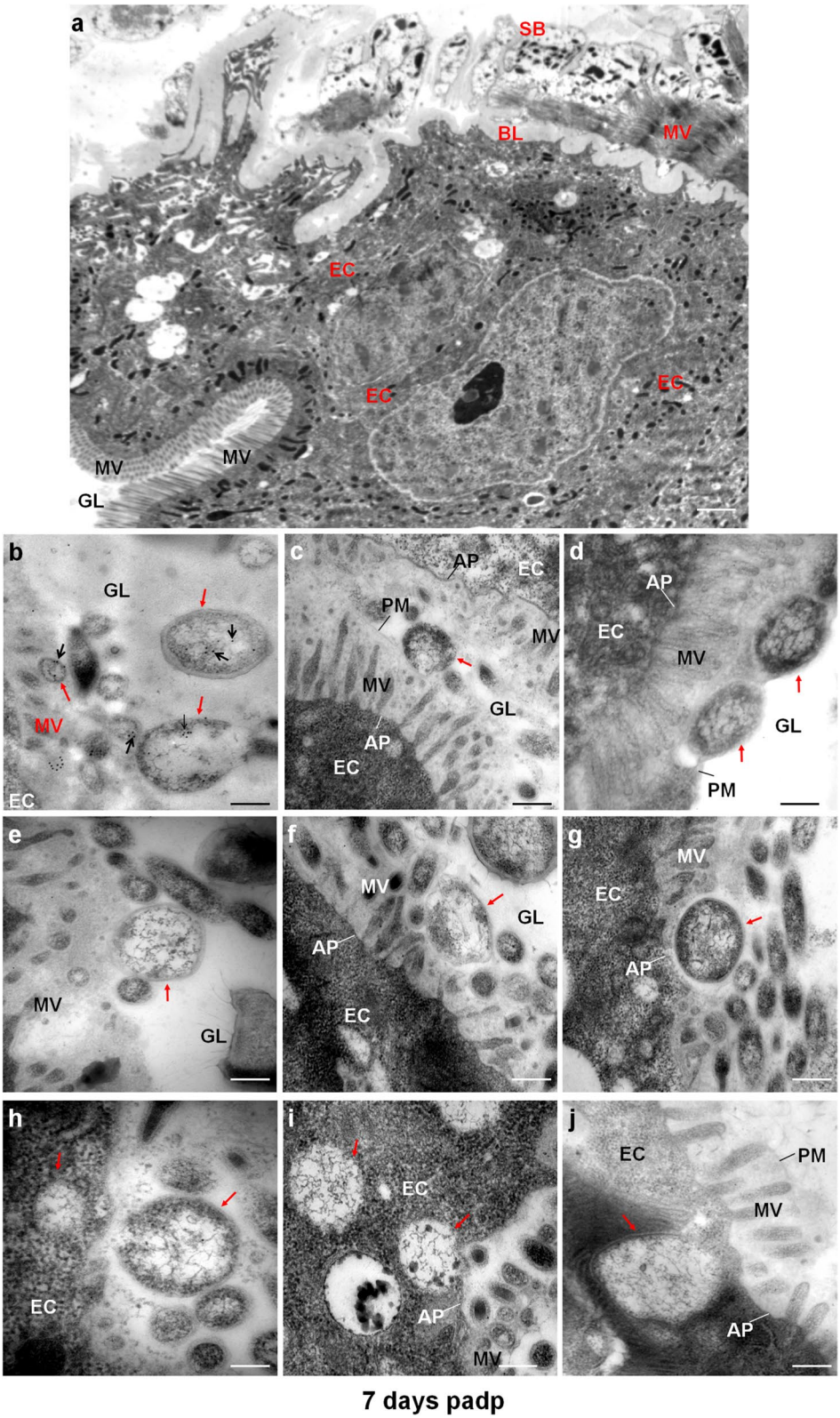

Fig. 3 (See legend on previous page.)

Phytoplasmas are transmitted in a persistent manner and undergo a propagative and multiplicative cycle in their insect vectors via colonization of the midgut and salivary glands. How phytoplasmas move into insect cells to propagate and spread has been a question of interest to phytopathologists for many years. What physical barriers do phytoplasmas encounter as they invade alimentary canal and salivary gland tissues? In the intestinal lumen, microvilli of leafhopper epithelial cells are thought to be protected by a perimicrovillar membrane (Ammar et al. 1985; Zhang et al. 2012). We observed that movement of ROLPs into epithelial cells would cause a disruption in the conformation of the perimicrovillar membrane and brush border formed by microvilli. More importantly, the entry of ROLPs into the intestinal epithelium is mediated by curvature of the apical plasmalemma and via endocytosis as seen with viruses (Wei and Li 2016). Once inside intestinal epithelial cells, ROLPs initiate an active propagation process to produce offspring by the division of mother cells. The basal lamina of hemipteran insects is a tightly interwoven and noncellular matrix, possibly constituting a substantial barrier for vector-borne pathogens including viruses (Wei and Li 2016; Jia et al. 2018). We observed that ROLPs could simply push the lamina matrix aside and slide along visceral muscles. ROLPs also simply cross the serosal barrier covered with visceral muscles to release into the hemolymph. The basal lamina covering salivary gland cells appears almost identical to that of the alimentary canal (Wayadande et al. 1997). The apical plasmalemma of saliva-stored cavities appears almost identical to that of the intestine. Also, the release of ROLPs into salivary cavities is mediated by inducing curvature of the apical plasmalemma. Our observations suggest that the first and last membrane barriers, the apical plasmalemmas in the alimentary canal and salivary glands, are the principal determinant of the ability of an insect species to transmit a phytoplasma (Fig. 7). Other noncellular matrixes including the perimicrovillar membrane, brush border, basal lamina, and serosal barrier may not act as the main barriers for phytoplasma dissemination (Fig. 7). Passage of phytoplasmas through these insect barriers requires specific interactions between surface-exposed proteins of phytoplasmas and vector components (Suzuki et al. 2006; Galetto et al. 2011; Boonrod et al. 2012; Yusa et al. 2014; Rashidi et al. 2015; Arricau-Bouvery et al. 2018; Abbà et al. 2019; Galetto et al. 2019). Our previous data show that actin filaments propel virus-induced tubules to facilitate movement across different membrane or tissue barriers in insect vectors (Chen et al. 2012, 2013; Jia et al. 2016; Mao et al. 2017). Amp and Imp of phytoplasmas have been shown to directly bind to host or insect actin microfilaments (Rashidi et al. 2015; Abbà et al. 2019). We thus deduce that insect factors such as actin filaments may provide enough power to allow phytoplasmas to squeeze and penetrate insect transmission barriers.

Phytoplasmas are an intriguing group of bacteria because they lack cell walls and cannot be cultured in vitro. Phytoplasmas must rely strictly on host phloem or insect vectors for propagation. Different from the classical binary fission used by most bacteria, ROLPs exploit an asymmetrical budding strategy to produce offspring in plant hosts and insect vectors. Some bacterial species form multiple intracellular offspring or use stalked budding to reproduce (Angert 2005; Eswara and Ramamurthi 2017). The stalked budding bacteria produce offspring by budding from the distal end of the stalk growing from mother cell surface (Eswara and Ramamurthi 2017). However, our observations found that ROLPs produced offspring by directly budding from mother cell surface. At the beginning of ROLP proliferation, a protrusion budded from the membrane of ROLP via the extension of the ROLP envelope. As growing, the cellular protrusion became enlarged for the onset of bud formation and ultimately separated from the mother cell. (Fig. 6 and Additional file 1: Figure S2). Those bud-like structures are also observed during propagation of other phytoplasmas (Hogenhout et al. 2008b). Due to the limitation of electron microscopy, we could not provide 3-dimensional (3D) images of ROLP replication structure. The development of 3D reconstruction technology, like electron tomography, would provide more details of phytoplasmas proliferation process in the future. Our findings reveal that phytoplasmas have evolved a unique asymmetrical reproduction mode. It will be interesting to dissect the molecular mechanisms regulating asymmetrical cell

(See figure on next page.)

Fig. 4 Electron micrographs showing the release of ROLPs from intestinal epithelium to salivary glands via the hemocoel of *R. dorsalis*. **a**, **b** Attachment of ROLPs to the basal lamina of the midgut. **b** is the enlarged image of boxed area in **a**. **c** Distribution of ROLPs in the space between the basal lamina and visceral muscle of the midgut. **d** Distribution of ROLPs in the space between the visceral muscle and the serosal barrier of the midgut. **e**–**h** Process for movement of ROLPs through the serosal barrier of the midgut. **i**, **j** Attachment of ROLPs to the basal lamina of salivary glands. **j** is the enlarged image of boxed area in **i**. **k**–**n** Process for movement of ROLPs through the basal lamina from the hemocoel into the salivary cell. **l** is the enlarged image of boxed area in **k**. BL, basal lamina; EC, epithelial cell; He, hemocoel; SB, serosal barrier; SC, salivary cytoplasm; VM, visceral muscle. Red arrows indicate ROLPs. Scale bars, 200 nm

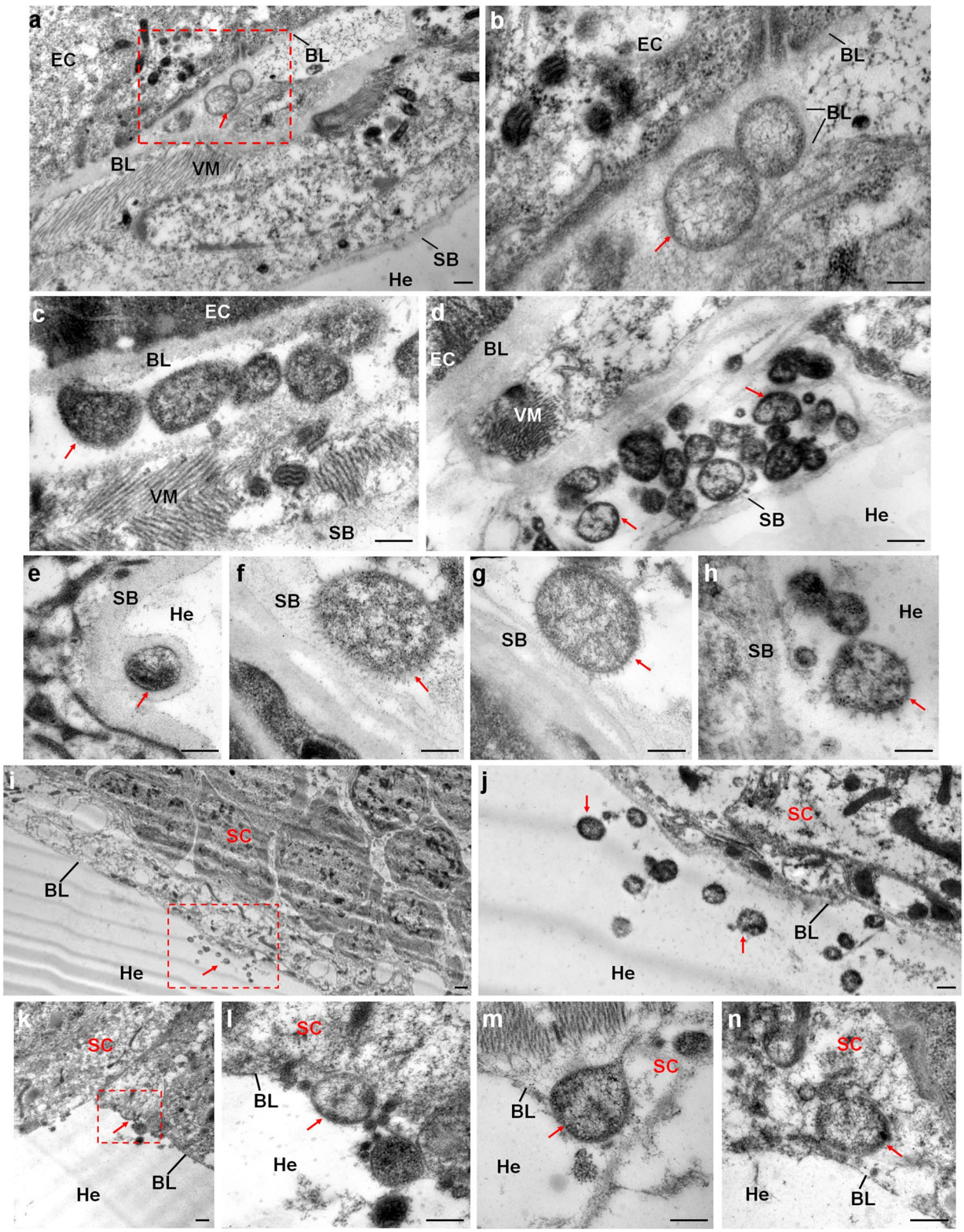

Fig. 4 (See legend on previous page.)

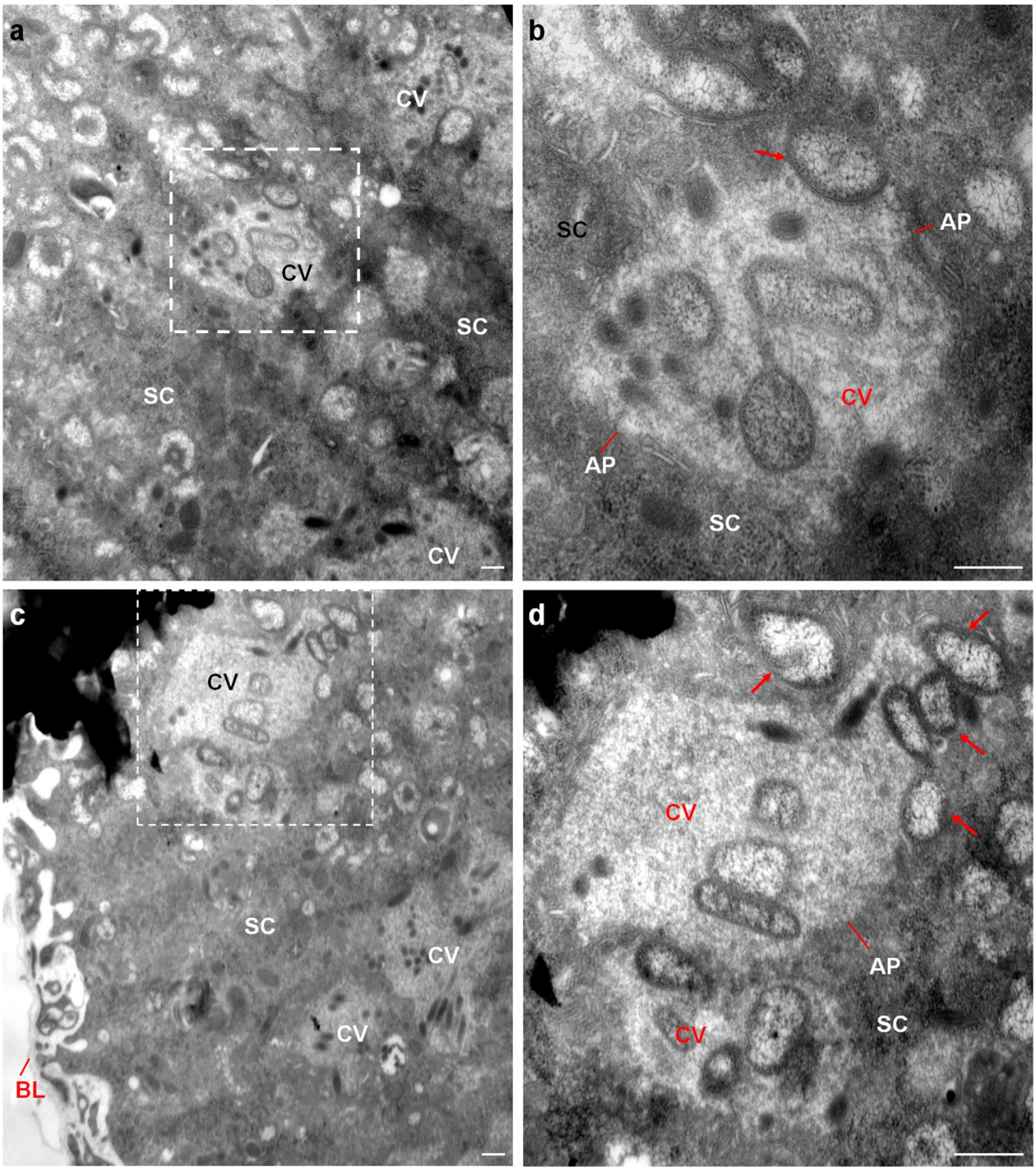

Fig. 5 Electron micrographs showing the release of ROLPs from the salivary cytoplasm into the cavities by crossing the apical plasmalemma of *R. dorsalis*. **a**–**d** Release of ROLPs into apical plasmalemma-lined cavities. **b** and **d** are the enlarged images of boxed areas in **a** and **c**, respectively. Arrows indicate the ROLPs which are directly squeezing or penetrating the apical plasmalemma into the cavities. AP, apical plasmalemma; BL, basal lamina; CV, cavity; SC, salivary cytoplasm. Scale bars, 200 nm

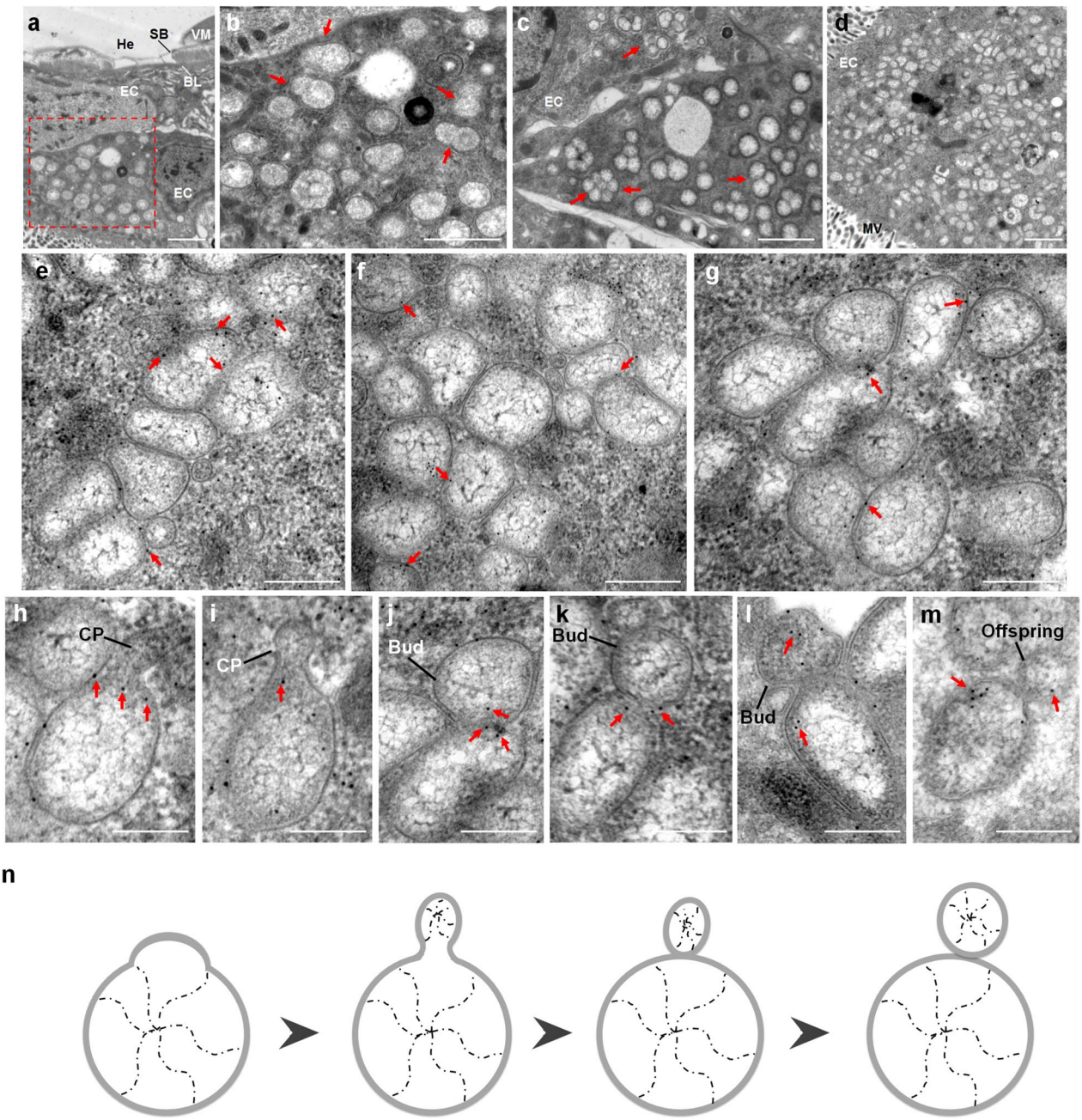

Fig. 6 Electron micrographs showing the multiplication of ROLPs in vector midgut epithelium to produce offspring. **a**, **b** One ROLP mother cell was reproducing one daughter cell (arrows). **b** is the enlarged image of boxed area in **a**. **c** More offspring were reproduced to form the grapelike clusters (arrows). **d** Abundant ROLP offspring were reproduced throughout the epithelial cytoplasm. **e**–**g** ROLPs of various sizes reacted with Imp-specific antibody. **h**–**m** The process for the budding strategy used by ROLPs to produce offspring. The cellular protrusion of a ROLP cell (**h**, **i**) was gradually enlarged to initiate the formation of a bud (**j**, **k**), and then offspring was produced by fission at their junction (**l**, **m**). **n** Proposed model of the budding reproduction strategy. ROLP-infected intestines shown in **e**–**m** were incubated with Imp-specific antibody and then with 15-nm gold particle-conjugated goat antibody against rabbit IgG as secondary antibody. Arrows indicate gold particles. BL, basal lamina; CP, cellular protrusion; EC, epithelial cell; He, hemocoel; MV, microvilli; SB, serosal barrier; VM, visceral muscle. Scale bars, 500 nm (**a**–**d**) and 200 nm (**e**–**m**)

division of phytoplasmas. In particular, the reproductive strategy of asymmetrical budding derived from cell protrusion confers an evolutionary advantage for the wall-less bacteria to produce more offspring than classical binary fission. Addressing these issues will also help to unravel the mechanisms underlying the striking morphological diversity of phytoplasmas.

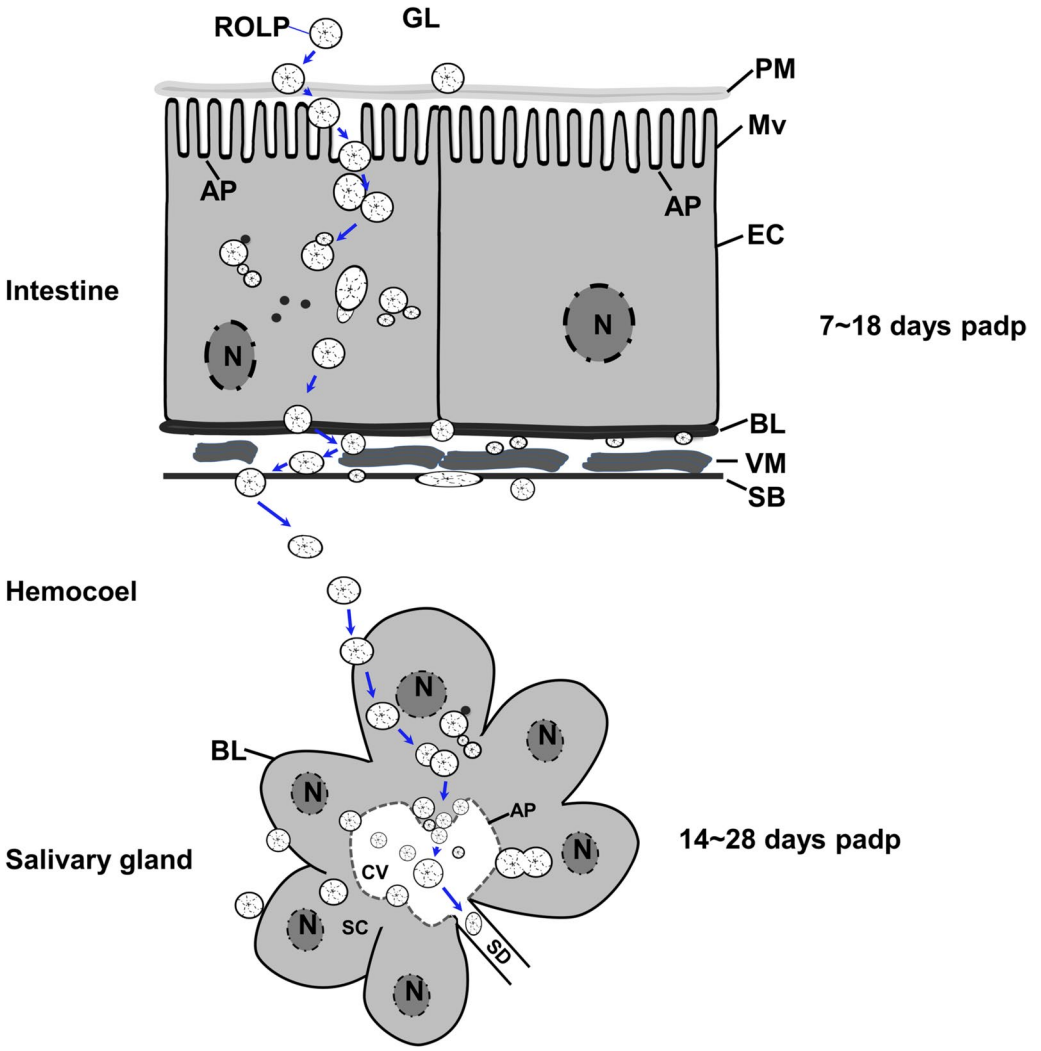

Fig. 7 Proposed model for ROLP entrance, multiplication, and release from insect vectors during transmission. ROLPs acquired from diseased rice plants sequentially traverse the perimicrovillar membrane, microvilli, and apical plasmalemma to enter the intestinal epithelium, where ROLPs produce abundant offspring via budding. The offspring successively traverse the basal lamina and serosal barrier to enter hemolymph. ROLPs in hemolymph then traverse the basal lamina of salivary cells to enter and produce offspring, which finally traverse the apical plasmalemma into saliva storage cavities. Finally, ROLPs are horizontally transmitted to rice phloem together with saliva during insect feeding on rice plants. Blue arrows indicate the process of phytoplasma spread. AP, apical plasmalemma; BL, basal lamina; CV, cavity; EC, epithelial cell; GL, gut lumen; Mv, microvilli; N, nucleus; PM, perimicrovillar membrane; SB, serosal barrier; SC, salivary cytoplasm; SD, salivary duct; VM, visceral muscle

Conclusions

In present study, we generated a specific antibody against Imp for the detection of ROLP in rice and *R. dorsalis.* We studied the distribution and multiplication of ROLP in rice and its infection route in *R. dorsalis* by qPCR and immune fluorescence labeling assay. Furthermore, we revealed the details of ROLP passing from the alimentary canal through the midgut into the haemocoel and colonizing salivary gland. Our results provide insights to better understand the infection mechanism of phytoplasma in host plant and insect.

Methods

Collection of ROLP-infected rice materials and ROLP acquisition by *R. dorsalis*

Rice plants with ROLD symptoms were obtained from an ROLP-infected field in Guangdong Province and were then confirmed by PCR test with ROLP-specific primers and grown in a growth chamber under a controlled environment. Healthy *R. dorsalis* populations were collected from Guangdong Province. The insects were screened, and a ROLP-free colony was reared on rice seedlings in clear containers in a controlled environment at 28 °C. In

all experiments involving ROLP-infected leafhoppers, second-instar *R. dorsalis* nymphs were fed on ROLP-infected rice plants for 4 days and then transferred to healthy rice seedlings. At different days padp, insects were collected for experiments.

Generation of antibodies against ROLP Imp protein

Different peptides of Imp protein were synthesized by GenScript@ Company. Rabbit polyclonal antibody against ROLP Imp protein was prepared as described previously (Wang et al. 2018). For one peptide, 0.7–1.0 mg peptides mixed with 1 mL Freund Adjuvant Complete (FCA; Pierce Biotechnology) were used as antigen to immunize rabbit for five times (once a week). IgGs were purified from polyclonal antibodies using protein A IgG binding buffer (Thermo, product number 21001) and IgG elution buffer (Thermo, product number 21004) and then conjugated directly with rhodamine (Invitrogen) according to the manufacturer's instructions.

Immunofluorescence labeling of frozen rice tissue sections

Rice leaves with ROLD symptoms (orange) were soaked in tissue freezing medium (Tissue-Tek O.C.T Compound) and frozen at −-20 °C overnight. Tissues were then sliced continuously using a freezing microtome (Leica CM1950) into 15 μm sections. The tissue sections were washed with 0.01 M phosphate-buffered saline (PBS) three times, fixed in 4% paraformaldehyde (PFA) at 4 °C for at least 8 h, and permeabilized at room temperature in 4% Triton X-100 for 6 h. Pre-treated samples were then immunolabeled with Imp-specific IgG directly conjugated with rhodamine (Imp-rhodamine) and examined using immunofluorescence microscopy. As controls, healthy rice leaves were sectioned and treated in the same way. All samples were observed using a Leica TCS SP5 inverted confocal microscope.

Immunofluorescence labeling of dissected organs of insect vectors

For visualizing the ROLP infection route in insect vectors, second instar nymphs of *R. dorsalis* were fed on diseased plants for 4 days and then transferred to healthy rice seedlings. At different days padp, the intestines, hemolymph, and salivary glands of 30 *R. dorsalis* individuals were dissected, fixed in 4% PFA for at least 8 h, and soaked in 4% Triton X-100 for 24 h at room temperature. The internal organs were then immunolabeled with Imp-rhodamine and the actin dye phalloidin-Alexa Fluor 647, and examined using immunofluorescence microscopy, as described previously (Wang et al. 2018). Healthy *R. dorsalis* individuals were dissected and treated following the above procedure as control. All samples were subjected to a Leica TCS SP5II confocal microscope.

Immunoelectron microscopy

At 7, 14, 21, and 28 days padp, a group of at least eight leafhoppers were collected and dissected for experiments. Meanwhile, ROLP-infected rice plants also were dissected for experiments. The different organs of *R. dorsalis* and rice plants were first fixed with 2% glutaraldehyde (Sigma, G5882) and 2% PFA (Sigma, 158,127) at 4 °C overnight, and then dehydrated in a graded series of ethanol up to 100% at − 20 °C. Dehydrated tissues were embedded with LR GOLD resin (Agar Scientific, AGR1284) at − 20 °C for 96 h under UV light. Three sections from each block were sliced using an ultramicrotome (Leica UC7). Ultrathin sections were incubated with Imp-specific antibody as the primary antibody and then treated with 15-nm gold particle-conjugated goat antibody against rabbit IgG as secondary antibody (Sigma-Aldrich), as described previously (Mao et al. 2017). All samples were subjected to electron microscopic observation (Hitachi H-7650).

ROLP titer quantification by qPCR and Western blotting

To determine the dynamics of ROLP genome copies in the *R. dorsalis* at 7, 14, 21, and 28 days padp, fifteen leafhoppers were collected and processed for experiments. Total genomic DNA was extracted from individual leafhopper adults using the CTAB method. ROLP genome copy number was quantified by absolute real-time qPCR using a SYBR Green PCR MasterMix kit (Promega, USA) in a Mastercycler Realplex4 real-time PCR system (Eppendorf, Germany) in accordance with the manufacturer's instructions. A primer set for 16S rRNA gene was used for ROLP detection (F: 5'AATGCGTAAATATAT GGAGG3', R: 5'TTGCGTACGTACTACTCAG3'). Ten-fold serial dilutions of purified plasmid (pTopo-ROLP16S rRNA) were used to generate a standard curve. For ROLP titer quantification, software was used to calculate the phytoplasma copy number in each sample using the Cq value of the sample and subsequently extrapolating on the standard curve. The copy numbers obtained were normalized for input amount of DNA using a qPCR assay for the *R. dorsalis* 18S rRNA gene. To determine the number of genomic units (copy number)/ng insect DNA, the phytoplasma copy number obtained for each sample was divided by the quantity (ng) of DNA in the same sample obtained from the standard curve for insect DNA.

Total proteins of ROLP-infected *R. dorsalis* (10 insects in one group) were extracted at 7, 14, 21, and 28 days padp, respectively. The accumulation of ROLP was

analyzed via Western blotting assays with Imp-specific antibody.

Statistical analysis

All data were analyzed for statistical differences using SPSS (version 19.0; SPSS, USA). Multiple comparisons of the means were conducted using a one-way analysis of variance and Tukey's honest significant difference (HSD) test at the $P < 0.05$ significance level.

Abbreviations

Amg: Anterior midgut; Amp: Antigenic membrane protein; Ap: Apical plasmalemma; Bl: Basal lamina; Cv: Cavity; Ec: Epithelial cell; Es: Esophagus; Fc: Filter chamber; Gl: Gut lumen; Imp: Immunodominant membrane protein; Mes: Mesophyll; Mmg: Middle midgut; Mt: Malpighian tubule; Mv: Microvilli; padp: Post-first access to diseased plants; PBS: Phosphate-buffered saline; PFA: Paraformaldehyde; Pm: Perimicrovillar membrane; Pmg: Posterior midgut; Pp: Phloem parenchyma; ROLD: Rice orange leaf disease; ROLP: Rice orange leaf phytoplasma; Sb: Serosal barrier; Sc: Salivary cytoplasm; Se: Sieve element; Sg: Salivary gland; St: Sieve tube; Ve: Vessel; Vm: Visceral muscle; VmpA: Variable membrane protein A.

Supplementary Information

The online version contains supplementary material available at https://doi.org/10.1186/s42483-022-00140-2.

Additional file 1: Figure S1. The alignment of Imp amino acid sequences from different phytoplasmas. The alignment of Imp amino acid sequences from ROLP (WP_071345699.1), maize bushy stunt phytoplasma (WP_069028105.1), aster yellows phytoplasma (WP_130427454.1), rapeseed phyllody phytoplasma (QKX95641.1), chrysanthemum yellows phytoplasma (WP_034172217.1), '*Chrysanthemum coronarium*' phytoplasma (WP_011160959.1), '*Elaeagnus angustifolia*' witches' broom phytoplasma (MBT1576836.1), porcelain vine witches' broom phytoplasma (WP_219475381.1), mulberry dwarf phytoplasma (WP_227807050.1), and hydrangea phyllody phytoplasma (WP_212775527.1) was performed using DNAMAN. The amino acid sequences of polypeptide for IMP2 antibody generation were indicated by red box**. Figure S2.** Electron micrographs showing multiplication of ROLPs in rice phloem to produce offspring. **a** ROLPs of various sizes associated with Imp-specific antibody. **b–d** Budding strategy used by ROLPs to produce offspring. Cellular protrusions of ROLPs (**b**) are gradually enlarged to initiate the formation of a bud (**c**). Offspring are then produced by fission at their junctions (**d**). CP, cellular protrusion. Scale bars, 100 nm.

Acknowledgements

We thank members of the Wei lab for stimulating discussions and technical assistance.

Authors' contributions

XZ and TW conceived and designed the study. XZ, ZJ (Zhenxi Ji), and ZH performed most of the experiments. YZ, HW, ZJ (Zhoumian Jiang), ZL, HC, and WC assisted with carrying out experiments. XZ and TW co-wrote the manuscript. All authors read and approved the final manuscript.

Funding

This research was supported by the National Natural Science Foundation of China (31871931), the Major International (Regional) Joint Research Program of China (31920103014), and Special Fund for Scientific and Technological Innovation of Fujian Agriculture and Forestry University (CXZX2020023A).

Availability of data and materials

Not applicable.

Declarations

Ethics approval and consent to participate

Not applicable.

Consent for publication

Not applicable.

Competing interests

The authors declare that they have no competing interests.

Author details

[1]State Key Laboratory of Ecological Pest Control for Fujian and Taiwan Crops, Institute of Plant Virology, Fujian Agriculture and Forestry University, Fuzhou 350002, Fujian, China. [2]Sanming Plant Protection and Plant Quarantine Station, Sanming 365000, Fujian, China.

Received: 7 July 2022 Accepted: 6 September 2022
Published online: 21 September 2022

References

Abbà S, Galetto L, Ripamonti M, Rossi M, Marzachì C. RNA interference of muscle actin and ATP synthase beta increases mortality of the phytoplasma vector *Euscelidius variegatus*. Pest Manag Sci. 2019;75:1425–34. https://doi.org/10.1002/ps.5263.

Ammar ED, Nault LR, Rodriguez JG. Internal morphology and ultrastructure of leafhoppers and planthoppers. In: Nault LR, Rodriguez JG, editors. Leafhoppers and planthoppers. New York: Wiley; 1985. p. 128–62.

Angert ER. Alternatives to binary fission in bacteria. Nat Rev Microbiol. 2005;3:214–24. https://doi.org/10.1038/nrmicro1096.

Arricau-Bouvery N, Duret S, Dubrana MP, Batailler B, Desqué D, Béven L, et al. Variable membrane protein A of flavescence dorée phytoplasma binds the midgut perimicrovillar membrane of *Euscelidius variegatus* and promotes adhesion to its epithelial cells. Appl Environ Microbiol. 2018;84:e02487-e2517. https://doi.org/10.1128/AEM.02487-17.

Boonrod K, Munteanu B, Jarausch B, Jarausch W, Krczal G. An immunodominant membrane protein (imp) of 'Candidatus Phytoplasma mali' binds to plant actin. Mol Plant-Microbe Interact. 2012;25:889–95. https://doi.org/10.1094/mpmi-11-11-0303.

Chen Q, Chen H, Mao Q, Liu Q, Shimizu T, Uehara-Ichiki T, et al. Tubular structure induced by a plant virus facilitates viral spread in its vector insect. PLoS Pathog. 2012;8: e1003032. https://doi.org/10.1371/journal.ppat.1003032.

Chen H, Zheng L, Jia D, Zhang P, Chen Q, Liu Q, et al. Rice gall dwarf virus exploits tubules to facilitate viral spread among cultured insect vector cells derived from leafhopper *Recilia dorsalis*. Front Microbiol. 2013;4:206. https://doi.org/10.3389/fmicb.2013.00206.

Eswara PJ, Ramamurthi KS. Bacterial cell division: nonmodels poised to take the spotlight. Annu Rev Microbiol. 2017;71:393–411. https://doi.org/10.1146/annurev-micro-102215-095657.

Firrao G, Andersen M, Bertaccini A, Boudon E, Bove JM, Daire X. '*Candidatus* Phytoplasma', a taxon for the wall-less, non-helical prokaryotes that colonize plant phloem and insects. Int J Syst Evol Micr. 2004;54:1243–55. https://doi.org/10.1099/ijs.0.02854-0.

Firrao G, Garciachapa M, Marzachì C. Phytoplasmas: genetics, diagnosis and relationships with the plant and insect host. Front Biosci. 2007;12:1353–75. https://doi.org/10.2741/2153.

Galetto L, Bosco D, Balestrini R, Genre A, Fletcher J, Marzachì C. The major antigenic membrane protein of "Candidatus Phytoplasma asteris" selectively interacts with ATP synthase and actin of leafhopper vectors. PLoS ONE. 2011;6: e22571. https://doi.org/10.1371/journal.pone.0022571.

Galetto L, Vallino M, Rashidi M, Marzachì C. Immunofluorescence assay to study early events of vector salivary gland colonization by phytoplasmas. Methods Mol Biol. 2019;1875:307–17. https://doi.org/10.1007/978-1-4939-8837-2_23.

Hogenhout SA, Ammar ED, Whitfield AE, Redinbaugh MG. Insect vector interactions with persistently transmitted viruses. Annu Rev Phytopathol. 2008a;46:327–59. https://doi.org/10.1146/annurev.phyto.022508.092135.

Hogenhout SA, Oshima K, Ammar ED, Kakizawa S, Kingdom HN, Namba S. Phytoplasmas: bacteria that manipulate plants and insects. Mol Plant Pathol. 2008b;9:403–23. https://doi.org/10.1111/j.1364-3703.2008.00472.x.

Jia D, Han Y, Sun X, Wang Z, Du Z, Chen Q, et al. The speed of tubule formation of two fijiviruses corresponds with their dissemination efficiency in their insect vectors. Virol J. 2016;13:174. https://doi.org/10.1186/s12985-016-0632-1.

Jia D, Chen Q, Mao Q, Zhang X, Wu W, Chen H, et al. Vector mediated transmission of persistently transmitted plant viruses. Curr Opin Virol. 2018;28:127–32. https://doi.org/10.1016/j.coviro.2017.12.004.

Jonson GB, Matres JM, Ong S, Tanaka T, Choi I-R, Chiba S. Reemerging rice orange leaf phytoplasma with varying symptoms expressions and its transmission by a new leafhopper vector—*Nephotettix virescens* distant. Pathogens. 2020;9:990. https://doi.org/10.3390/pathogens9120990.

Koinuma H, Maejima K, Tokuda R, Kitazawa Y, Yamaji Y. Spatiotemporal dynamics and quantitative analysis of phytoplasmas in insect vectors. Sci Rep. 2020;10:4291. https://doi.org/10.1038/s41598-020-61042-x.

Konnerth A, Krczal G, Boonrod K. Immunodominant membrane proteins of phytoplasmas. Microbiology. 2016;162:1267–73. https://doi.org/10.1099/mic.0.000331.

Kumari S, Nagendran K, Rai AB, Singh B, Rao GP, Bertaccini A. Global status of phytoplasma diseases in vegetable crops. Front Microbiol. 2019;10:1349. https://doi.org/10.3389/fmicb.2019.01349.

Lee IM, Davis RE, Gundersen-Rindal DE. Phytoplasma: phytopathogenic mollicutes. Annu Rev Microbiol. 2000;54:221–55. https://doi.org/10.1146/annurev.micro.54.1.221.

Lee IM, Gundersen-Rindal DE, Davis RE, Bottner KD, Marcone C, Seemüller E. '*Candidatus* Phytoplasma asteris', a novel phytoplasma taxon associated with aster yellows and related diseases. Int J Syst Evol Microbiol. 2004;54:1037–48. https://doi.org/10.1099/ijs.0.02843-0.

Li S, Hao W, Lu G, Huang J, Liu C, Zhou G. Occurrence and identification of a new vector of rice orange leaf phytoplasma in South China. Plant Dis. 2015;99:1483–7. https://doi.org/10.1094/pdis-12-14-1243-re.

Mao Q, Liao Z, Li J, Liu Y, Wu W, Chen H, et al. Filamentous structures induced by a phytoreovirus mediate viral release from salivary glands in its insect vector. J Virol. 2017;91:e00265-e317. https://doi.org/10.1128/jvi.00265-17.

Namba S. Molecular and biological properties of phytoplasmas. Proc Jpn Acad Ser B Phys Biol Sci. 2019;95:401–18. https://doi.org/10.2183/pjab.95.028.

Neriya Y, Maejima K, Nijo T, Tomomitsu T, Yusa A, Himeno M, et al. Onion yellow phytoplasma P38 protein plays a role in adhesion to the hosts. FEMS Microbiol Lett. 2014;361:115–22. https://doi.org/10.1111/1574-6968.12620.

Ong S, Jonson GB, Calassanzio M, Rin S, Chou C, Oi T, et al. Geographic distribution, genetic variability and biological properties of rice orange leaf phytoplasma in Southeast Asia. Pathogens. 2021;10:169. https://doi.org/10.3390/pathogens10020169.

Pagliari L, Musetti R. Phytoplasmas: an introduction. Methods Mol Biol. 2019;1875:1–6. https://doi.org/10.1007/978-1-4939-8837-2_1.

Pagliari L, Martini M, Loschi A, Musetti R. Looking inside phytoplasma-infected sieve elements: a combined microscopy approach using *Arabidopsis thaliana* as a model plant. Micron. 2016;89:87–97. https://doi.org/10.1016/j.micron.2016.07.007.

Rashidi M, Galetto L, Bosco D, Bulgarelli A, Vallino M, Veratti F, et al. Role of the major antigenic membrane protein in phytoplasma transmission by two insect vector species. BMC Microbiol. 2015;15:193. https://doi.org/10.1186/s12866-015-0522-5.

Rossi M, Samarzija I, Šeruga-Musić M, Galetto L. Diversity and functional importance of phytoplasma membrane proteins. In: Bertaccini A, Oshima K, Kube M, Rao G, editors. Phytoplasmas: Plant Pathogenic Bacteria-III. Singapore: Springer; 2019. https://doi.org/10.1007/978-981-13-9632-8_5.

Sugio A, Hogenhout SA. The genome biology of phytoplasma: modulators of plants and insects. Curr Opin Microbiol. 2012;15:247–54. https://doi.org/10.1016/j.mib.2012.04.002.

Suzuki S, Oshima K, Kakizawa S, Arashida R, Jung HY, Yamaji Y, et al. Interaction between the membrane protein of a pathogen and insect microfilament complex determines insect-vector specificity. Proc Natl Acad Sci USA. 2006;103:4252–7. https://doi.org/10.1073/pnas.0508668103.

van Bel AJE. Sieve Elements: The favourite habitat of phytoplasmas. In: R. Musetti, and L. Pagliari, editors. Phytoplasmas: methods and protocols. New York: Springer; 2019. https://doi.org/10.1007/978-1-4939-8837-2_19.

Valarmathi P, Rabindran R, Velazhahan R, Suresh S, Robin S. First report of rice orange leaf disease phytoplasma (16 SrI) in rice (*Oryza sativa*) in India. Australas Plant Dis. 2013;8:141–3. https://doi.org/10.1007/s13314-013-0117-7.

Wang H, Wang J, Xie Y, Fu Z, Wei T, Zhang X. Development of leafhopper cell culture to trace the early infection process of a nucleorhabdovirus, rice yellow stunt virus, in insect vector cells. Virol J. 2018;15:72. https://doi.org/10.1186/s12985-018-0987-6.

Wayadande AC, Baker GR, Fletcher J. Comparative ultrastructure of the salivary glands of two phytopathogen vectors, the beet leafhopper, *Circulifer tenellus* (Baker), and the corn leafhopper, *Dalbulus maidis* DeLong and Wolcott (Homoptera: Cicadellidae). Int J Insect Morphol Embryol. 1997;26:113–20. https://doi.org/10.1016/S0020-7322(97)00009-3.

Wei T, Li Y. Rice reoviruses in insect vectors. Annu Rev Phytopathol. 2016;54:99–120. https://doi.org/10.1146/annurev-phyto-080615-095900.

Weintraub PG, Beanland L. Insect vectors of phytoplasmas. Annu Rev Entomol. 2006;51:91–111. https://doi.org/10.1146/annurev.ento.51.110104.151039.

Zhang F, Zhang C, Dai W, Zhang Y. Morphology and histology of the digestive system of the vector leafhopper *Psammotettix striatus* (L.) (Hemiptera: Cicadellidae). Micron. 2012; 43: 725–38. https://doi.org/10.1016/j.micron.2012.01.004